*Materials Transactions*, Vol. 44, No. 7 (2003) pp. 1488 to 1493

EXPRESS REGULAR ARTICLE

# Formation of Nanocrystalline Structure in Steels by Air Blast Shot Peening

Minoru Umemoto, Yoshikazu Todaka and Koichi Tsuchiya

*Department of Production System Engineering, Toyohashi University of Technology, Toyohashi 441-8580, Japan*

The formation of nanocrystalline structure (NS) on the surface of bulk steel samples by a particle impact and air blast shot peening techniques was studied. Nanocrystalline layers with several microns thick were successfully fabricated by these methods. The nanocrystalline layers produced in the present study have extremely high hardness and separated from adjacent deformed morphology region with sharp boundaries. By annealing, nanocrystalline layers showed slow grain growth without recrystallization. Those characteristics are similar to those observed in the NS produced by ball milling and a ball drop deformation. It was suggested that to produce NS by deformation a large strain is a necessary condition and a high strain rate and low temperature are favorable conditions.

(Received March 28, 2003; Accepted June 9, 2003)

***Keywords:*** *severe plastic deformation (SPD), nanostructure, shot peening, particle impact, steels*

## 1. Introduction

Nanocrystalline materials (grain size smaller than 100 nm) have attracted considerable scientific interests in the past decade. Various severe plastic deformation (SPD) methods have been proposed to produce nanocrystalline materials, such as ball milling (BM),[1,2] high pressure torsion (HPT),[3] ultrasonic shot peening[4–6] and a ball drop deformation (BD).[7,8] Among these, extensive works have been performed on BM due to its easiness to install in laboratories and applicability to essentially all classes of materials. From our previous BM experiments in steels,[9–12] it was found that the nanocrystalline regions have the following characteristics: 1) with grains smaller than 100 nm and low dislocation density interior of grains, 2) separated from deformed morphology region with clearly defined boundaries, 3) extremely high hardness (8–13 GPa), 4) dissolution of cementite when it exists and 5) no recrystallization and slow grain growth by annealing. Since BM is not suitable process to study the nanocrystallization mechanism due to the complex deformation mode and high contamination, BD in which a ball with weight was dropped onto specimens was employed. By BD test, nanocrystalline surface layer was found to be produced on bulk steel samples. The amount of strain necessary to produce nanocrystalline structure (NS) and the effect of deformation temperature was investigated. However, BM or BD is not suitable process to produce nanocrystalline materials industrially.

The purpose of the present study is to demonstrate new SPD techniques, *i.e.* particle impact (PI) and air blast shot peening processes, to produce nanocrystalline regions on the surface of bulk steel samples. The nanocrystalline regions formed by these techniques were compared with those in ball milled or ball dropped samples previously studied.

## 2. Experimental Procedures

The materials used in the present study were a silicon steel of Fe–3.29Si (Fe–3.29Si–0.01Mn in mass% hereafter), a 590 MPa class high tensile strength steel (Fe–0.05C–1.29Mn) and an eutectoid carbon steel of Fe–0.80C (Fe–0.80C–0.20Si–1.33Mn) with pearlite or spheroidite structures. The pearlite structure in Fe–0.80C was obtained by austenitizing the samples at 1223 K for 1.8 ks and then kept at 873 K for 0.3 ks to transform to pearlite. To obtain spheroidite structure in Fe–0.80C, specimens were austenitized at 1173 K for 3.6 ks and quenched into water to obtain martensite. Such specimens were tempered at 983 K for 79.2 ks.

The apparatus of PI and shot peening are shown in Fig. 1. PI experiment (Fig. 1(a)) was done by a high-pressure light gas gun which can accelerate particles in a desired speed. Helium was used as particle carrier gas. The bore of 4.2 mm in inner diameter and 3.9 m in length was used. A bearing steel (Fe–1Cr–1.5Cr in mass%) ball with 4 mm in diameter was chosen as a projectile and was accelerated to the speed of 120 m/s. Specimens of 30 × 30 × 3 mm were mounted at the end of bore and impacted 1 to 200 times in air. The experiments were done either at room temperature or at liquid nitrogen ($LN_2$) temperature. Air blast shot peening (Fig. 1(b)) was performed to the specimen of 15 mm × 15 mm × 2 mm using cast steel shot (Fe–1.0C–1.3Si–1.0Mn in mass%, HV 8 GPa, $<\phi$50 μm, shot speed 190 m/s) from a

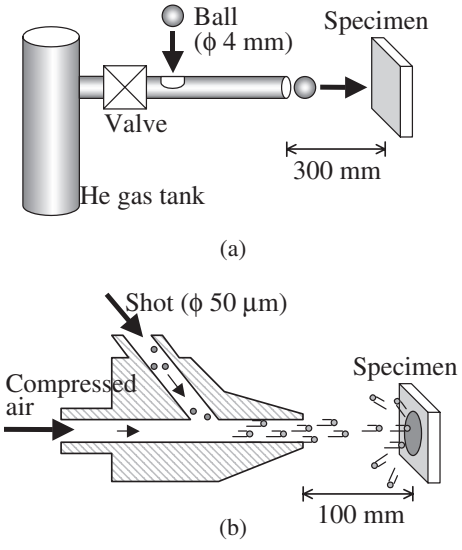


Fig. 1 Apparatus used in the present study. (a) a particle impact apparatus (b) an air blast shot peening machine.

distance of 100 mm. The processing duration was in the range from 10 to 60 s which corresponds to the coverage of 1000 to 6000%. (The coverage is the area fraction of specimen surface deformed by shots. Coverage larger than 50% was given multiplying shot peening time by % coverage per second estimated at 50% coverage.)

Specimens were characterized by scanning electron microscope (SEM, JEOL JSM-6300), transmission electron microscope (TEM, Hitachi H-800 working at 200 kV) and microvickers hardness tester (MVK-G1 with an applied load of 9.8 N for 10 s). Specimens for SEM observations were etched by 5% Nital. Thin foils for TEM observations were prepared by cutting a specimen parallel to the surface into discs of 3 mm in diameter using a wire spark machine and dimpling from bottom side which is followed by electropolishing.

## 3. Results

### 3.1 Particle impact experiment

Figure 2(a) shows a Fe–0.80C pearlitic specimen after 8 times of particle impacts at $LN_2$ temperature. The specimen was pre-strained by cold rolling (82%). The dark contrast layers of several 10 μm thickness are produced on the top or sub-surface of the specimen. From the Vicker's indentation marks shown in Fig. 2(b) (an enlarged micrograph of Fig. 2(a)), the microhardness of the dark contrast layer was measured as 9.5 GPa which is substantially higher than the surrounding work-hardened region (4.3 GPa). Figure 2(c) is another area of the same specimen showing the enlarged picture of the boundary between the dark contrast region and the work-hardened region. It is seen that cementite lamellae are invisible in the dark contrast region, indicating the dissolution of cementite in this region. This is quite different from the simple work-hardened pearlite structure where the reduction of interlamellar spacing or bending of cementite lamellae are observed. These characteristics are same with those observed in the nanocrystalline region produced by ball milling or a ball drop test as reported previously.[7–12] Thus it is concluded that NS can be produced by a present particle impact deformation. It is considered that NS is produced in the region where the most severe deformation occurred. In the case of PI, the degree of deformation may not be largest at the surface of the specimen because of the friction between the specimen and ball. It was noticed that the nanocrystalline layer produced by PI is slightly thinner than those observed in specimens after BD. The experiment done at room temperature under the same condition required a larger number of impacts than at $LN_2$ temperature to form nanocrystalline region. This suggests that low temperature deformation enhances the formation of nanocrystalline regions.

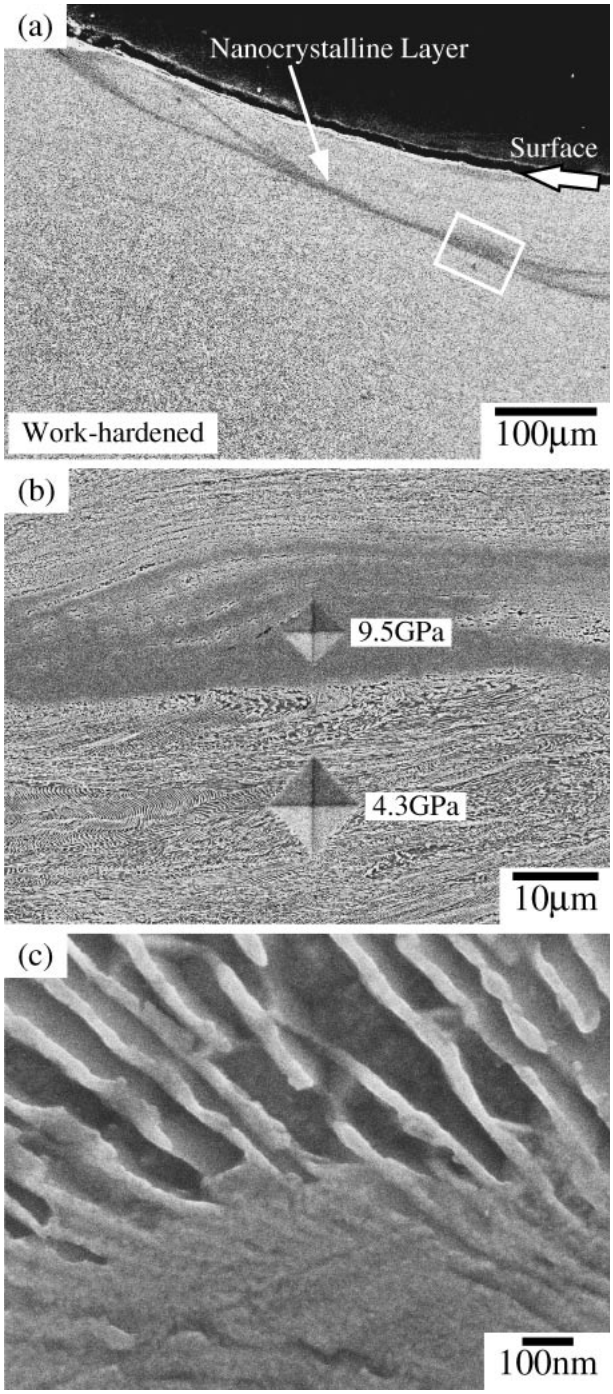


Fig. 2 SEM micrographs of nanocrystalline layers formed in pre-strained (82% cold rolled) Fe–0.80C specimen with pearlite structure after 8 times of particle impacts at $LN_2$ temperature. (a) overview, (b) enlarged images of (a) showing the hardness and (c) another area of the same specimen.

### 3.2 Air blast shot peening experiment

Figure 3(a) shows a cross sectional SEM micrograph of Fe–0.05C–1.29Mn high tensile strength steel (initial structure is fine grained (about 5 μm) ferrite) after shot peened for 10 s. Two distinctive regions can be seen. One is the bright contrast region near surface which has the hardness of 6.8 GPa. This region was confirmed as nanocrystalline region by TEM. Another is the dark contrast region which has the hardness of 2.6 GPa. From the elongated grain boundaries, it is clear that this region is in work-hardened condition. After annealed at 873 K for 3.6 ks (Fig. 3(b)), nanocrystalline region did not show any detectable change while the work-hardened regions just adjacent to nanocrystalline region showed recrystallization. In the shot peened specimen, it is considered that the amount of strain is largest at the top surface and decreases with the depth. Nanocrystallization can occur within several microns from the top surface and below this is the work-hardened region. The boundaries between the

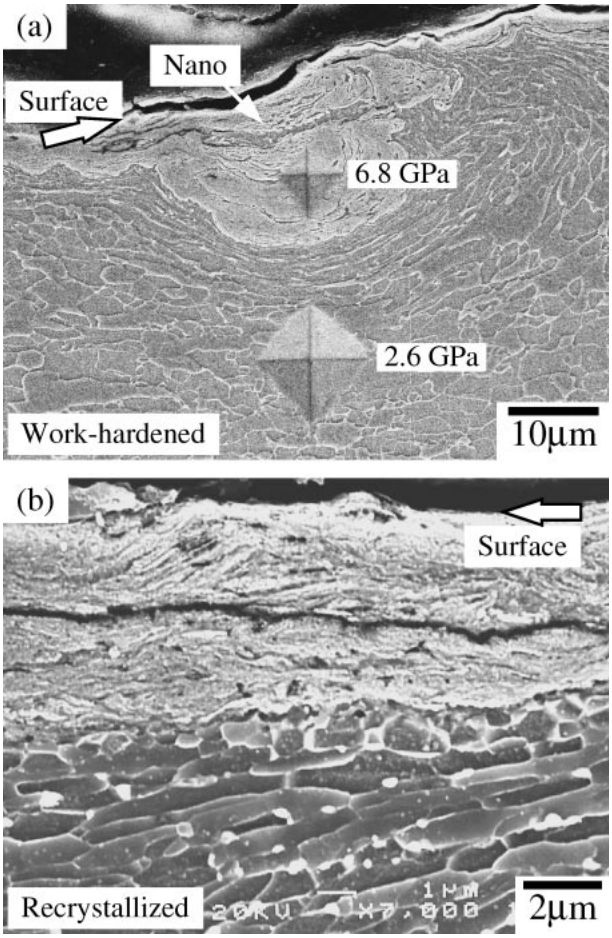


Fig. 3 SEM micrographs of Fe–0.05C–1.29Mn high tensile strength steel after shot peened for 10 s. (a) as shot peened and (b) annealed at 873 K for 3.6 ks after shot peening.

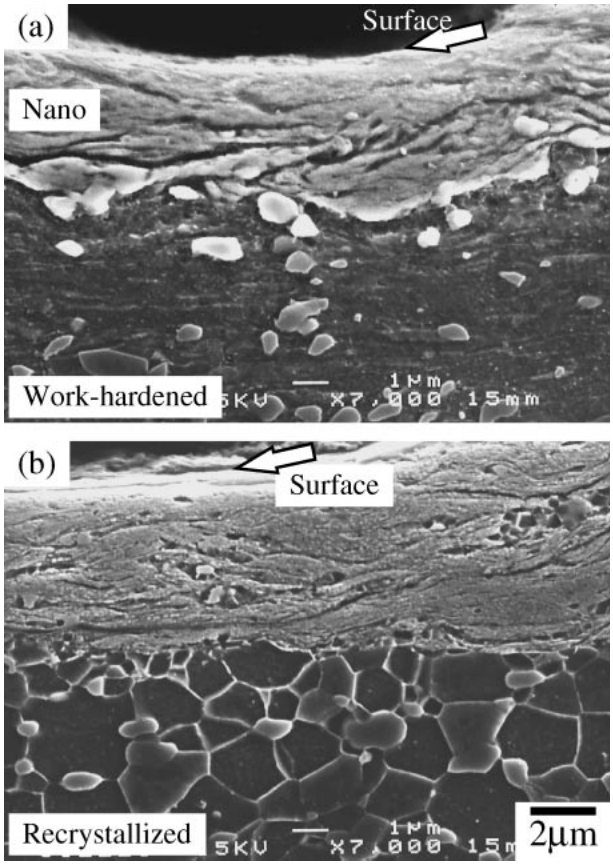


Fig. 4 SEM micrographs of the nanocrystalline regions formed in pre-strained (82% cold rolling) Fe–0.80C specimen with spheroidite structure by shot peened for 10 s. (a) As shot peened and (b) annealed at 873 K for 3.6 ks after shot peening.

nanocrystalline and work-hardened regions are sharp similar to those observed in ball milled powder or ball dropped specimens.[7–12] Recrystallization can occur in the area received sufficient degree of deformation. It was noted that the morphology of nanocrystalline region is quite similar to that produced by BM.[9–12]

Figure 4(a) shows a nanocrystalline surface layer formed in Fe–0.80C specimen (pre-strained 84% by cold rolling) with spheroidite structure after shot peening. Before shot peening, the spheroidized cementite particles with diameter about 0.5 μm were uniformly distributed in the ferrite matrix. After shot peening, cementite particles are visible in the work-hardened region but not visible in the nanocrystalline surface layer. This indicates that the dissolution of cementite takes place in the nanocrystalline layer similar to that observed in ball milled or ball dropped specimens. Figure 4(b) shows a SEM micrograph after annealing at 873 K for 3.6 K. It is seen that the nanocrystalline surface layer did not show any detectable change while the sub-surface work-hardened region showed recrystallization. In this case, the specimen is pre-strained and recrystallization took place in the whole specimen except for the nanocrystalline layer. This annealing behavior of the nanocrystalline and work-hardened regions is similar to those observed in ball milled,[11,12] ball dropped[8] and particle impacted Fe–0.80C specimens with spheroidite structure.

The development of nanocrystalline surface layers with peening duration was studied using Fe–0.80C specimens (pre-strained 81% by cold rolling) with spheroidite structure. Figure 5 shows the SEM micrographs after 10 and 60 s of shot peening. It is seen that the area fraction and thickness of the nanocrystalline layer increased with peening time. In the

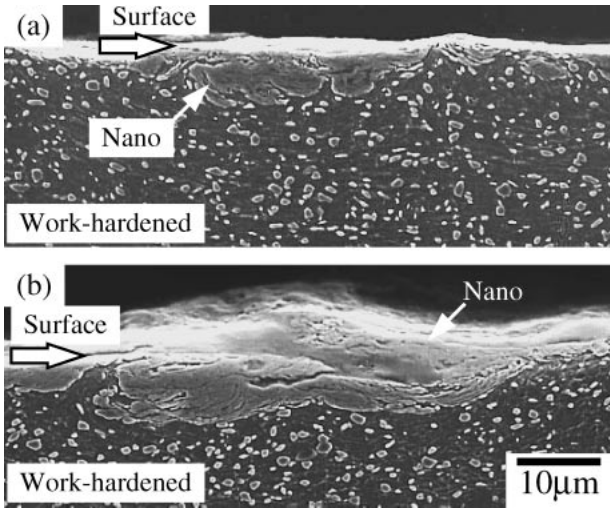


Fig. 5 Effect of peening duration on the formation of nanocrystalline surface layer. Pre-strained (81% cold rolled) Fe–0.80C specimens with spheroidite structure were shot peened for (a) 10 s and (b) 60 s.

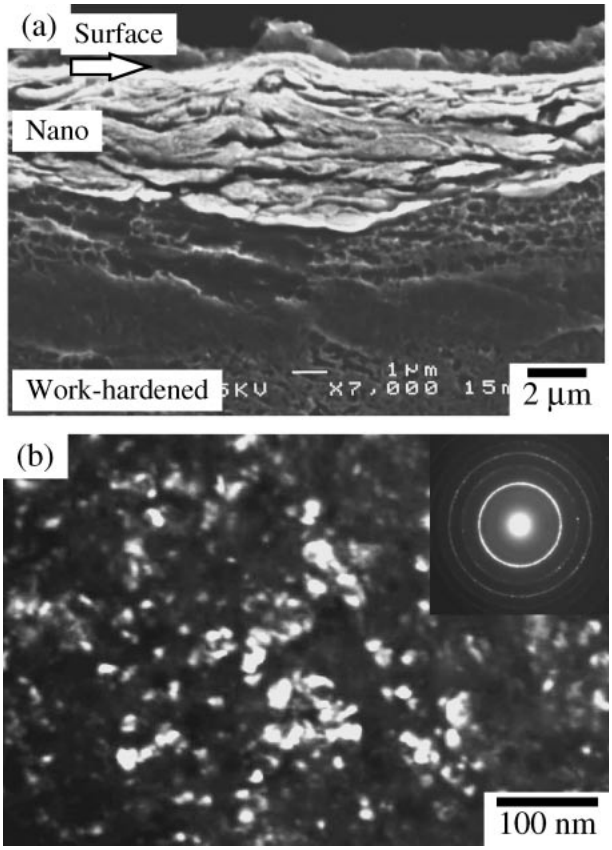


Fig. 6 Microstructures of shot peened Fe–3.29Si specimen. (a) SEM micrograph after shot peened for 10 s and (b) TEM and SAD pattern ($\phi$1.2 μm in aperture size) of nanocrystalline region of the specimen shot peened for 60 s.

conventional shot peening, the coverage is usually less than a few 100% and a detectable volume of nanocrystalline region could not be formed. This is the reason why nanocrystallization was not realized in the conventional shot peening.

Figure 6(a) shows nanocrystalline region formed in Fe–3.29Si specimen by 10 s of shot peening. The sharp boundary between nanocrystalline and work-hardened regions is seen, which is similar to that observed in ball milled Fe–3.29Si powder. Figure 6(b) is the dark field (DF) image and selected area diffraction (SAD) pattern of the top surface region of Fe–3.29Si specimen shot peened for 60 s. The DF image shows that the ferrite grain size is less than 20 nm, and the SAD pattern indicates that the ferrite grains have random orientations.

Regarding the mechanism of the above microstructural evolution, the idea associated with a thermally induced martensitic transformation[13] is most widespread. It is assumed that owing to the severe plastic deformation, temperature higher than $A_1$ (1000 K) arises at the surface, leading to austenite formation. After deformation, subsequent rapid cooling of the surface layer causes the martensite transformation. However, since bcc structure in Fe–3.29Si alloy is stable up to its melting point, it is clear that the formation of nanocrystalline layer is not associated with thermally induced martensite.

## 4. Discusion

In the present study, it was found that NS can be produced by PI and air blast shot peening. The production of nanocrystalline surface layer by air blast shot peening has considerable importance since air blast shot peening is a popular process in industries and it can produce nanostructured surface layer with a high productivity. Industrial application of this new technique is expected especially to upgrade the traditional engineering materials. To optimize the known processes or develop new processes to produce NS, it is important to understand the necessary and favorable deformation conditions to produce NS. In the previous and present studies, BM,[1,2,9–12] BD,[7,8] PI and air blast shot peening are demonstrated to be possible processes to generate NS. The deformation conditions common to these processes are considered to be a large strain and a high strain rate. However, the numerical values of these are hard to measure in these processes. Here, reviewing previous related works, these values are discussed.

### 4.1 Amount of strain

Large strains seem to be the most important factor to produce NS. The reported amount of strain applied to obtain NS (grain size less than 100 nm) varies from 7 to 31 depending on the deformation techniques and materials employed.

The amount of strain can be measured well in drawing and torsion experiments. Langford and Cohen[14] observed microstructure of severely drawn iron wear strained up to $\varepsilon = 6$. At $\varepsilon = 6$ the flow stress was 1.4 GPa and mean transverse linear-intercept cell sizes was 90 nm. If 1.4 GPa is simply due to grain boundary strengthening, the size of grains (with medium and large misorientation) is estimated to be 260 nm according to the Hall-Petch relationship for iron[10] ($\sigma$[GPa] $= 0.12 + 20d^{-1/2}$, $d$ in nm). Extrapolating their flow stress vs strain data, the strain which gives the flow stress corresponding to $d = 100$ nm (2.1 GPa) is estimated to be $\varepsilon = 12$. Tashiro[15] measured the flow stress of drown iron wire straind up to $\varepsilon = 11.5$. The flow stress increased linearly with strain and became 3 GPa at strain of 11. The flow stress corresponding to $d = 100$ nm (2.1 GPa) is achieved at $\varepsilon = 7$. Although the grains size of the drown wire was not measured, grain size less than 100 nm is believed to be accomplished. The difference in the amount of strain to obtain the flow stress of 2.1 GPa between Langfor *et al.*[14] ($\varepsilon = 11.8$) and Tashiro[15] ($\varepsilon = 7$) may arise from the difference in the drawing conditions applied. The experiment of high pressure torsion straining in iron was carried out by Valiev *et al.*[3] Armco iron was subjected to torsion straining up to 10 turns ($\varepsilon = 360$) under a pressure of 7 GPa at a strain rate of 0.5 $s^{-1}$. They reported that the grain size decreased and hardness increased with increasing strain. After 3 turns ($\varepsilon = 108$) the hardness reaches 4.5 GPa and tends to reach a steady state. The grain size about 100 nm was obtained after 5 turns ($\varepsilon = 180$) at which the hardness was 4.6 GPa. The microhardness of 4.6 GPa corresponds to the flow stress of 1.53 GPa from the usual approximate relation between microhardness and flow stress, namely Hv $= 3\sigma$. The reported hardness is too low to consider that the size of grains

with large misorientation is reduced to 100 nm in their experiment. Similar torsion experiment has been done by Kaibyshev *et al.*[16] in Fe–3%Si under the pressure of 9 GPa. After straining to $\varepsilon = 31$ (0.5 turn), grains are refined to 120–200 nm and the microhardness increased to 7.2 GPa. From the microhardness it can be considered that the grain size less than 100 nm was achieved. The hardness measured was 3.6 GPa at $\varepsilon = 4.3$ and 7.2 GPa at $\varepsilon = 31$, then the grain refinement to $d = 100$ nm (Hv = 6.3 GPa) was accomplished at strain $4.3 < \varepsilon < 31$.

The amount of strain to produce nanocrystalline structure was also estimated in a BD test and sliding wear test, although with less accuracy. In a BD test of pearlitic steel, Umemoto *et al.*[17] estimated the amount of strain and atrain rate from the shear band with NS produced by one time of ball drop. The total equivalent true strain was estimated to be 7.3 (pre-strain of 80% cold rolling ($\varepsilon = 1.9$), 8.1 in shear strain ($\varepsilon = 4.7$) and 52% uniform compression ($\varepsilon = 0.7$) by a ball drop test). The strain rate during BD was calculated to be $1.3 \times 10^4\ s^{-1}$ from the amount of strain of 5.4 by a ball drop test (8.1 in shear strain ($\varepsilon = 4.7$) and 52% uniform compression ($\varepsilon = 0.7$)) divided by the ball-to-specimen contact time ($4.3 \times 10^{-4}$ s). In sliding wear test, Heilmann *et al.*[18] obtained nanograined layer of 3–30 nm on the top surface of Cu block. The estimated plastic shear strain at the surface was ~11.4 and an upper limit of the strain rate was $3.7 \times 10^3\ s^{-1}$. Hughes and Hansen[19] studied the nanostructures in Cu produced by sliding. The amount of strain to reach $d = 100$ nm is estimated from the relationship between grain size (or grain boundary spacing) and strain as 8.

Summarizing the above mentioned studies, the minimum amount of strain necessary to produce nanocrystalline structure is considered to be around 7–8, although it depends on materials, microstructure, deformation techniques and deformation conditions employed.

### 4.2 Strain rate

High strain rate deformation may not be a necessary condition to produce NS since NS has been produced in a wide spread range of strain from 0.5 to $10^4\ s^{-1}$. However, high strain rates deformation probably enhance the formation of NS due to the following several reasons: 1) increase flow stress, 2) increase work-hardening at a given strain, 3) increase dislocation multiplication rate, and 4) promote lattice rotation and increase misorientation angle.

It has been well known that flow stress of metals increase with strain rate.[20] Higher flow stresses activate a larger number of slip systems and promote grain subdivision and subgrain rotation. Greater hardening has been observed in metals strained at higher strain rates when compared at equal strain. The iron samples subjected to high-intensity shock waves of explosive origin (strain rate $\sim 10^6\ s^{-1}$) showed much greater hardening than those deformed by rolling.[21] Thus it is expected that high strain rate deformation reduce the necessary amount of strain to produce NS. High strain rate deformation promote smaller cells or subgrains due to higher dislocation multiplication rate and hence higher dislocation density than those deformed at low strain rates. The rotation of cells or grains is induced by the deformation of different slip systems in adjacent cells or grains. Since high strain rate deformation activate more slip systems due to high flow stress, high strain rates are favorable to obtain randomly oriented fine grains with large misorientation.

As the strain rate is increased the deformation tends more and more towards an adiabatic state. The generated heat rise the temperature of sample and accelerates recovery and grain growth. In an extreme case the increase in strain rate results in the increase in grain size.[22] Thus to obtain grain refinement by high strain rate deformation, care should be taken for cooling during and post deformation so that the temperature of the specimen will not rise so much.

### 4.3 Other deformation factors

Other favorable conditions for the formation of NS are considered as follows; 1) low temperature deformation, 2) repetitive or cyclic deformation, 3) multidirectional deformation, 4) impurities and/or alloying elements, 5) second phase, 6) hydrostatic pressure.

The suppression of recovery by preventing dislocation motion favors the formation of NS. Low deformation temperature and hydrostatic pressure slow down self-diffusion and, consequently, delay recovery kinetics. Applying a large accumulative strain by cyclic or repetitive deformation with a small strain at each time is effective to suppress recovery since specimens are cooled during each strain interval. Multidirectional deformation activates multi slip systems and increases dislocation interaction frequencies which leads to the development of fine cells. Impurities and/or alloying elements, precipitates and second phase retard dislocation motion by pinning or dragging effect and suppress recovery.

The deformation conditions to produce NS was discussed reviewing various previous works. At present there is no conclusive answer which can specify the necessary and sufficient conditions to produce NS. However, examining various available data obtained using various deformation techniques, it is becoming clear that there is a common deformation condition to produce NS. Uncertainties in the numerical values in the amount of strain, strain rate and other deformation conditions are mainly due to the difficulties to produce uniformly deformed nanostructured bulk samples. Further studies on NS formation with various different deformation techniques are expected.

## 5. Conclusions

Particle impact and air blast shot peening techniques were demonstrated to be new severe plastic deformation processes effective to produce nanocrystalline structure (NS). The formation of nanocrystalline regions was confirmed by TEM observations, microhardness measurements and annealing experiments. It is confirmed that the nanocrystalline regions formed by these techniques have extremely high hardness and showed no recrystallization but slow grain growth by annealing. These characteristics are similar to those produced by ball milling and a ball drop deformation. The necessary deformation condition to produce NS common in various severe plastic deformation processes is a strain larger than about 7. High strain rate and low temperature are suggested to be favorable deformation conditions to produce NS.

## Acknowledgements

This study is financially supported in part by the Grant-in-Aid by the Japan Society for the Promotion of Science (No. 14205103).

## REFERENCES

1) J. S. C. Jang and C. C. Koch: Scr. Metall. Mater. **24** (1990) 1599–1604.
2) H. J. Fecht, E. Hellstern, Z. Fu and W. L. Johnson: Metall. Trans. **21A** (1990) 2333–2337.
3) R. Z. Valiev, Y. V. Ivanisenko, E. F. Rauch and B. Baudelet: Acta Mater. **44** (1996) 4705–4712.
4) G. Liu, S. C. Wang, X. F. Lou, J. Lu and K. Lu: Scr. Mater. **44** (2001) 1791–1795.
5) N. R. Tao, M. L. Sui, J. Lu and K. Lu: NanoStructured Mater. **11** (1999) 433–440.
6) N. R. Tao, Z. B. Wang, W. P. Tong, M. L. Sui, J. Liu and K. Lu: Acta Mater. **50** (2002) 4603–4616.
7) M. Umemoto, B. Huang, K. Tsuchiya and N. Suzuki: Scr. Mater. **46** (2002) 383–388.
8) M. Umemoto, X. J. Hao, T. Yasuda and K. Tsuchiya: Mater. Trans. **43** (2002) 2536–2542.
9) M. Umemoto, Z. G. Liu, K. Masuyama, X. J. Hao and K. Tsuchiya: Scr. Mater. **44** (2001) 1741–1745.
10) J. Yin, M. Umemoto, Z. G. Liu and K. Tsuchiya: ISIJ Int. **41** (2001) 1389–1396.
11) Y. Xu, Z. G. Liu, M. Umemoto and K. Tsuchiya: Metall. Mater. Trans. **33A** (2002) 2195–2203.
12) Y. Xu, M. Umemoto and K. Tsuchiya: Mater. Trans. **43** (2002) 2205–2212.
13) W. Osterle, H. Rooch, A. Pyzalla and L. Wang: Mater. Sci. Eng. **A303** (2001) 150–157.
14) G. Langford and M. Cohen: Trans. ASM **62** (1969) 623–638.
15) H. Tashiro: Doctor thesis at Tohoku Univ. (1992).
16) R. Kaibyshev, I. Kazakulov, T. Sakai and A. Belyakov: *Proc. of Int. Symp. on Ultrafine grained steels*, (The Iron and Steel Institute of Japan, 2001) pp. 152–155.
17) M. Umemoto, Y. Todaka and K. Tsuchiya: J. Metastable and Nanocrystalline Mater. **15–16** (2003) 193–198.
18) P. Heilmann, W. A. T. Clark and D. A. Rigney: Acta Metall. **31** (1983) 1293–1305.
19) D. A. Hughes and N. Hansen: Phys. Rev. Lett. **87** (2001) 135503-14.
20) J. D. Campbell and W. G. Ferguson: Philos. Mag. **21** (1970) 63–82.
21) G. E. Dieter: *Response of metals to high velocity deformation*, (P. G. Shewman and V. F. Zackay (eds), Interscience, New York, 1961) pp. 409–445.
22) N. Tsuji, T. Toyoda, Y. Minamino, Y. Koizumi, T. Yamane, M. Komatsu and M. Kiritani: Mater. Sci. Eng. A (2002) in press.